COLUMBIA/EINSTEIN OBSERVATIONS OF GALACTIC X-RAY SOURCES

Knox S. Long
Columbia Astrophysics Laboratory

The imaging proportional counter (IPC) has been used to observe a large variety of galactic X-ray sources in the first months of operation of the Einstein satellite. We will now discuss some of those observations, namely, those carried out for Columbia University. The observations to date fall into three broad categories: pre-main-sequence stars in the Orion Nebula, isolated main- and post-main-sequence stars, and supernova remnants.

The Orion Nebula is the newest, large region of active star formation in the Galaxy. Prior to the launch of the Einstein satellite, a relatively weak (10^{33} erg s^{-1}) source of X-ray emission had been localized in the Orion Nebula, coincident with the four OB stars which comprise the Trapezium (Bradt and Kelley 1979 and references therein). The first of several planned observations of the Orion region was carried out early this year, and the results are shown in Figure 1. The strongest source in the field is coincident with the Trapezium, but in addition there are many other sources, 22 at a confidence level of 4 σ or greater. These sources have typical luminosities of 10^{31} ergs s^{-1}. Several of these sources may be identified with relatively bright O or B stars in the field. However, a detailed analysis carried out by Ku and Chanan (1979) revealed that, as a group, the Orion sources are strongly correlated with the positions of bright nebular variables, as cataloged by Kukarkin et al. (1968, 1971, 1974, 1977). Nebular variables are a heterogeneous class of pre-main-sequence stars, which include T Tauri variables with UV Ceti-like flare stars, which exhibit irregular light curves. A large number of nebular variables have been cataloged in the Orion Nebula. A Monte Carlo simulation indicates that 5 $\pm$ 5 (2 σ error) stars would be expected to fall within the error circles of the X-ray positions, whereas the 22 error circles (excluding the Trapezium) contain a total of 25 bright ($m_V < 15$) nebular variables. The test implies that either the nebular variables are X-ray sources or that they are tracers of X-ray activity, presumably because both are associated with star formation. In fact, we cannot exclude the second possibility, based on the observations to date. However, in the absence of another suitable class of X-ray sources and because X-ray emission from pre-main-sequence stars had been previously predicted (den Boggende et al. 1976; Kuhi 1964; Ulrich 1978; Mullan 1976), we favor the hypothesis that nebular variables are indeed X-ray emitters, a new class of X-ray object. This is a hypothesis that can be resolved by carrying out extended observations with the high resolution imager (HRI).

The first main-sequence star detected at X-ray wavelengths was the Sun. Its X-ray luminosity is highly variable but is typically 10^{26} ergs s^{-1}. X-ray emission from the Sun arises from the plasma which constitutes the solar corona and is created by the dissipation of mechanical energy in the atmosphere of the Sun. This mechanical energy arises from convection in the outer envelope of the Sun. Model calculations and some observational data [notably the decrease in the strength of He λ10830 emission in early type stars (Zirin 1978)] indicate that convection disappears in stars earlier than spectral type F. Hence it was somewhat surprising to detect X-ray emission from β Cen A, a nearby B1 giant as indicated in Figure 2. The X-ray luminosity of β Cen A is approximately 8×10^{30} ergs s^{-1}. The fraction of the total energy radiated from the star as X-rays is approximately 10^{-7}, which is similar to the fractional flux radiated at X-ray wavelengths by the Sun. Assuming that convection does indeed disappear in early type stars, the solution to understanding the X-ray emission from these objects presumably is connected to the massive stellar winds associated with O and B stars which have maximum velocities of order 10^8 km s^{-1}. The X-ray luminosity of β Cen A is a small fraction of the energy which is available from such a wind. Since model calculations (Nelson and Hearn 1978) indicate that such winds are unstable, it may not be surprising, in retrospect, that X-rays are emitted. In the data which have been analyzed at Columbia, approximately 30 main- and post-main-sequence stars have been detected, many serendipitously. The detection of X-ray emission from a large number of normal stars makes possible, for the first time, a systematic study of the X-ray emitting properties of normal stars which do, after all, constitute the dominant form of mass in the Galaxy.

Tycho's supernova was first observed in 1572. A type I supernova, its optical emission peaked at magnitude of -4.0 ± 0.3 (van den Bergh 1970). The remnant was first observed at X-ray wavelengths by Friedman, Byram, and Chubb (1967). This SNR was the first remnant observed as part of an extensive survey of SNR being conducted at Columbia. The image shown in Figure 3 represents the result of that 2500 sec pointing. The important features of the image are the bright shell which can be traced over three-fourths of the circumference and the apparent break in the shell in the southeast. The peak brightness in the shell is approximately 2.5 times that of the center. The total counting rate from the remnant was approximately 20 counts s^{-1}. The diameter of the remnant is approximately 8' which should be compared to the full width at half maximum of the point response function approximately 1.5'. The edges of the remnant are sharp except possibly in the southeast, consistent with the angular resolution of the IPC. Assuming a distance of 3 kpc (Woltjer 1972), this means that the shock has a width of 1 pc or less. The radius of the remnant in the southeast appears approximately 20 percent greater than elsewhere. Since the remnant has most likely swept up substantially more matter from the interstellar medium (ISM) than was ejected from the star in the SN

explosion, the Sedov solutions to SNR evolution may be applied. In order to explain the difference in expansion rates, the density encountered by the shock in the southeast must have been approximately half that encountered in other directions.

A comparison between the X-ray and radio contours is shown in Figure 4. The two maps are quite similar. (The radio map of Strom and Duin 1973 has somewhat finer resolution.) The X-ray and radio shells have the same radii within the errors and both lie inside the optical filaments. There are differences however. For example, the radio contours peak in the northeast whereas X-ray emission peaks in the northwest. The polarization of radio emission is relatively lower in the northeast than in other parts of the shell (Strom and Duin 1973), which may be due to depolarization in the increased density of that portion of the radio shell. Preliminary analyses of the X-ray spectra of various regions of the remnant indicate that the increased flux in the shell is due to density and line-of-sight effects rather than differences in the temperature of a hot plasma.

A second SNR observed in the early months of operation of the Einstein satellite is W28 (Fig. 5). X-ray emission had not been detected prior to the launch of the Einstein satellite. This remnant which has a diameter of approximately 40' fills a single IPC field, and more observations will be required to understand the details of its structure. The X-ray luminosity of W28 is approximately 10^{35} ergs s^{-1} if the distance is taken to be 3 kpc (Woltjer 1972). Unlike Tycho's SNR, the X-ray picture of W28 shows no evidence of shell structure. The surface brightness appears relatively featureless and peaks near the center of the remnant, well inside the nonthermal radio shell which was observed by Shaver and Goss (1970). The optical picture obtained by van den Bergh et al. (1973) shows sharp optical filaments and considerable nebulosity. The lack of a distinct X-ray shell, and the X-ray luminosity and the size of W28 indicate that this SNR is at a much more advanced stage of evolution than Tycho's SNR.

An important feature of the map of the Einstein observation of Tycho's SNR is that there appears to be no bright object at the center of the remnant, as might be expected had a hot neutron star formed when the SN occurred approximately 400 years ago. If a neutron star had been created, it would not have moved from the central region of the remnant since pulsars are known to have typical velocities of 200 km s^{-1} (Helfand and Tademaru 1977), whereas the shock front in Tycho's SNR has expanded with a mean velocity of 9000 km s^{-1}. As discussed by Helfand, Chanan, and Novick (1979), the X-ray data obtained for Tycho's SNR can be used to place a limit of approximately 2×10^6 K for the temperature of a 10 km neutron star radiating as a blackbody. Since all models of SNR which produce neutron stars indicate that the neutron stars will be formed at temperatures of approximately 10^{10} K,

the lack of enhanced emission from the center of Tycho's SNR implies either that no pulsar was formed or that it cooled rapidly. The cooling curves for various neutron star models have been summarized recently by Tsuruta (1979). Figure 6 is abstracted from her paper. The solid curves represent envelopes for neutron star cooling in which the center of the neutron star does not contain pion condensates; the dashed curves represent the envelope for cooling curves which do contain pion condensates. In models with pion condensates, the neutron star cools rapidly at early times because of the additional channels for neutrino cooling provided by the existence of pions. The X-ray observations of Tycho's SNR seem to require pion condensates, if, in fact, a pulsar were formed.

A serious problem arises in studying the generic properties of supernova remnants using a sample of galactic remnants because the distance and the line-of-sight absorption to many SNR is poorly known. One way to circumvent this problem is to survey the properties of SNR in external galaxies. Our nearest neighbor galaxy is the Large Magellanic Cloud, an irregular galaxy with a prominent bar. In the tradition of Henrietta Leavitt, we therefore set out to study the properties of SNR in the LMC as part of a more general survey of that galaxy. A number of SNR had been identified in the LMC prior to the launch of the Einstein satellite, based on the existence of nonthermal radio sources in regions exhibiting filamentary structure in Hα and strong (S II) emission.

To date, observations of 10 of the 14 SNR and SNR candidates listed by Mathewson and Clarke (1973, hereafter MC) have been carried out. An initial analysis of these data has been completed (Long and Helfand 1979). Eight of the 10 SNR were detected, the first SNR ever detected at X-ray wavelengths in an external galaxy. Six of the remnants have 0.5-3.0 keV luminosities exceeding 10^{36} ergs s^{-1}. Also observed were sources coincident with two additional objects which were a part of a less rigorous list of SNR candidates compiled by Davies, Elliott, and Meaburn (1976; hereafter DEM).

A spectacular example of emission from SNR in the LMC is shown in Figure 7. Both bright sources there are SNR. The remnant in the southeast (lower left), known as N49, is approximately twice as bright as the remnant in the northwest, known as (N49). There is, in fact, an Hα bridge which joins N49 and (N49) and a break in the optical shell in the direction of (N49). As a result, MC suggested that (N49) was not a separate SNR but was perhaps the result of a massive compact object ejected from N49. The detection of (N49) as a separate X-ray source seems to confirm (N49) as a separate SNR. Evans et al. (1979) have recently reported the detection of a giant gamma-ray burst whose position is coincident with N49. Data obtained before and after the gamma-ray burst indicate no change in the X-ray luminosity of N49, but if the gamma-ray burst was located there, it had a peak luminosity of approximately 5×10^{44} ergs s^{-1} (Mazets et al. 1979). (The constraints

placed on the burst by the Einstein observations of this field are discussed by Helfand and Long 1979).

A plot of the X-ray luminosity of LMC supernova remnants versus their optical diameters is shown in Figure 8. Optical diameters for the plot were obtained from the compilation of MC (1973), where possible, or from the list of DEM (1976) if they were not in the MC survey. The determination of the optical diameters of SNR is somewhat subjective, and for remnants included in both lists, there are considerable differences in the optical diameters derived by MC and DEM.[1] Since the optical counterparts of N157B and N158A are yet to be established, the diameters for these sources were estimated by MC on the basis of a radio surface brightness (Σ - D) relation for the other SNR in their survey. There appears to be a considerable range in luminosity for SNR of the same general size; however, a general trend is evident for luminosities to decrease as the radius exceeds 30 pc, as it is for similar plots of SNR in our own Galaxy. The Sedov solution for a symmetric blast wave propagating into a uniform density medium allows one to solve for the age of the remnant and the ratio of the energy of the initial explosion to the ambient density n_o of the ISM, given the radius and temperature of the remnant. Following Gorenstein and Tucker (1976), we have estimated n_o directly from the X-ray luminosity and temperature, assuming that X-ray emission from the SNR originates in a shell of uniform density 4 n_o. This degree of compression corresponds to conditions behind a strong shock in a gas having a ratio of specific heats equal to 5/3. Ages derived from this analysis range from just over 1000 years to 20 000 years and are reasonably consistent with the observed optical expansion rates. As expected, the calculated explosion energies are not dependent upon remnant size or age; they range from 0.8 to 3.4 $\times$ 10^{50} ergs, with a mean of 2 $\times$ 10^{50} ergs and are similar to energies derived from galactic remnants when the same model is applied (Gorenstein and Tucker 1976). However, the ISM densities derived from the model are highly correlated with observed remnant diameters, as shown in Figure 9, ranging from 0.047 to 11 cm^{-3}, which is inconsistent with the simple blast wave model in which n_o should be independent of the diameter. McKee and Ostriker (1977) have developed a detailed theory of supernova shock waves expanding into a tenuous ISM ($n_o > 10^{-2.5}$ cm^{-3}), studded with small clouds ($n_o > 10$ cm^{-3}).

---

1. Work is now in progress on a more accurate way of determining the optical diameters from HRI observations of the SNR in the LMC. Results obtained since this paper was presented indicate that the optical diameters of MC considerably underestimate the X-ray diameters of the brighter remnants at least.

The clouds have only a small effect on the dynamics of the shock. X-ray emission in this model is dominated by matter which is evaporated from the cool, relatively dense clouds. The importance of the evaporation decreases as a function of time, and hence McKee and Ostriker (1977) predict an apparent density decrease similar to what is observed.

The initial survey of the LMC is now approximately half complete. In addition to the known SNR, approximately 30 other sources have been detected. These sources include the emission nebula 30 Doradus, shown in Figure 10. The emission nebula is the extended source in the center. It has a luminosity of approximately 10^{36} ergs s^{-1}. This nebula resembles in some aspects the Orion Nebula; both are hydrogen rich regions with active star formation. However, according to Bok (1966), if 30 Doradus were placed at the distance of the Orion Nebula, it would cover almost 25 degrees of the sky and cast permanent shadows on the Earth. One of the challenges presented by the Einstein observations is to understand emission from this region, which is 10^3 brighter than the Trapezium. Other sources in this field include LMC X-1, which is distorted because of its position near the edge of the field, and the SNR N157B and N158A, as well as several unidentified sources.

In concluding, let me note that work has only just begun on analyzing the first observations of the LMC, as well as of SNR and normal and pre-main-sequence stars. The surveys themselves are only partially complete. Many more and often deeper observations are planned. However, I think that the implications of the current observations are clear. The horizon of X-ray astronomy has expanded with the Einstein satellite to include not only rare and exotic objects, such as supernova remnants and pulsars, but stars of all types and many other objects as well. In that sense, X-ray astronomy has changed from a separate discipline with its own parochial interests to a field in which X-ray observations serve as a tool to understand sources of general interest to astrophysicists.

We at Columbia wish to join other members of the HEAO-2 Consortium in thanking the many individuals at the NASA George C. Marshall Space Flight Center, the NASA Goddard Space Flight Center, the NASA John F. Kennedy Space Center, the NASA Headquarters, and in private industry without whom the Einstein Observatory would not have become a reality. This work was supported by the National Aeronautics and Space Administration under contract NAS8-30753. This paper is Columbia Astrophysics Laboratory Contribution No. 179.

REFERENCES

Bok, B. J., 1966, Ann. Rev. Astron. Astrophys., 4, 95.

Bradt, H. V., and Kelley, R. L., 1979, Astrophys. J. (Letters), 228, L33.

Davies, R. D., Elliott, K. H., and Meaburn, J., 1976, Mem. Roy. Astron. Soc., 81, 89 (DEM).

den Boggende, A. J. F., Mewe, R., Gronenschild, E. H. B. M., Heise, J., and Grindlay, J. E., 1978, Astron. Astrophys., 62, 1.

Evans, D., Klebesadel, R., Baros, J., Cline, T., Desai, U., Teegarden, B., and Pizzichini, G., 1979, I.A.U. Circ., No. 3356.

Friedman, H., Byram, E. T., and Chubb, T. A., 1967, Science, 156, 374.

Gorenstein, P., and Tucker, W. H., 1976, Ann. Rev. Astron. Astrophys., 14, 373.

Helfand, D. J., Chanan, G. A., and Novick, R., 1979, Nature, in press.

Helfand, D. J., and Long, K. S., 1979, preprint.

Helfand, D. J., and Tademaru, E., 1977, Astrophys. J., 216, 842.

Ku, W. H.-M., and Chanan, G. A., 1979, Astrophys. J. (Letters), in press.

Kuhi, L. V., 1964, Astrophys. J., 140, 1409.

Kukarkin, B. V., et al., 1968, General Catalogue of Variable Stars (Moscow: Publishing House of the Academy of Sciences, USSR); Suppls. 1971, 1974, 1977.

Long, K. S., and Helfand, D. J., 1979, Astrophys. J. (Letters), in press.

Mathewson, D. S., and Clarke, J. N., 1973, Astrophys. J., 180, 725 (MC).

Mazets, E. P., Golenetskii, S. V., Il'inskii, V. N., Aptekar', R. L., and Guryan, Yu. A., 1979, Nature, in press.

McKee, C. F., and Ostriker, J. P., 1977, Astrophys. J., 218, 148.

Mullan, D. J., 1976, Astrophys. J., 207, 289.

Nelson, G. D., and Hearn, A. G., 1978, Astron. Astrophys., 65, 223.

Strom, R. G., and Duin, R. M., 1973, Astron. Astrophys., 25, 351.

Shaver, P. A., and Goss, W. M., 1970, Australian J. Phys. Astrophys. Suppl., 14, 77.

Tsuruta, S., 1979, Phys. Reports, in press.

Ulrich, R. K., 1978, in Protostars and Planets, ed., T. Gehrels (Tucson: Univ. of Arizona Press).

van den Bergh, S., 1970, Nature, 225, 503.

van den Bergh, S., Marscher, A. P., and Terzian, Y., 1973, Astrophys. J. Suppl., 26, 19.

Woltjer, L., 1972, Ann. Rev. Astron. Astrophys., 10, 129.

Zirin, H., 1978, Astrophys. J., 208, 414.

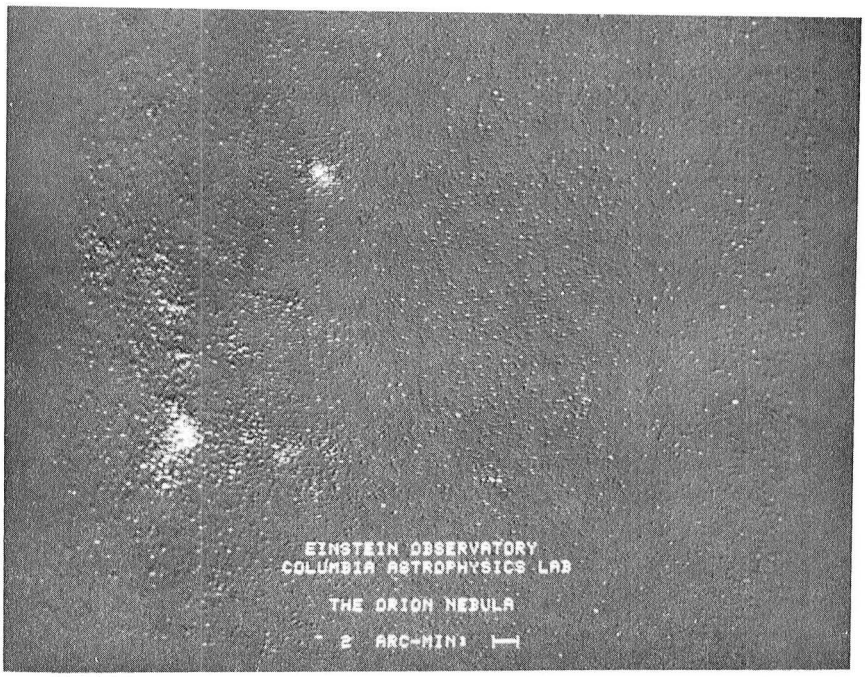

Figure 1. The results of an initial observation of the Orion region with the IPC. The bright source in the southeast is the Trapezium.

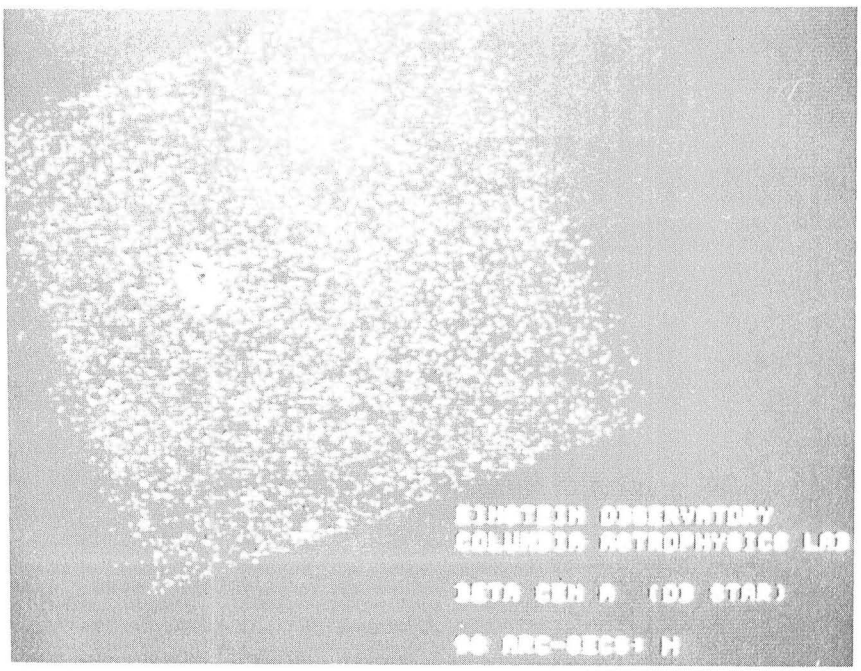

Figure 2. The B supergiant β Cen A as observed in a short observation with the Einstein IPC.

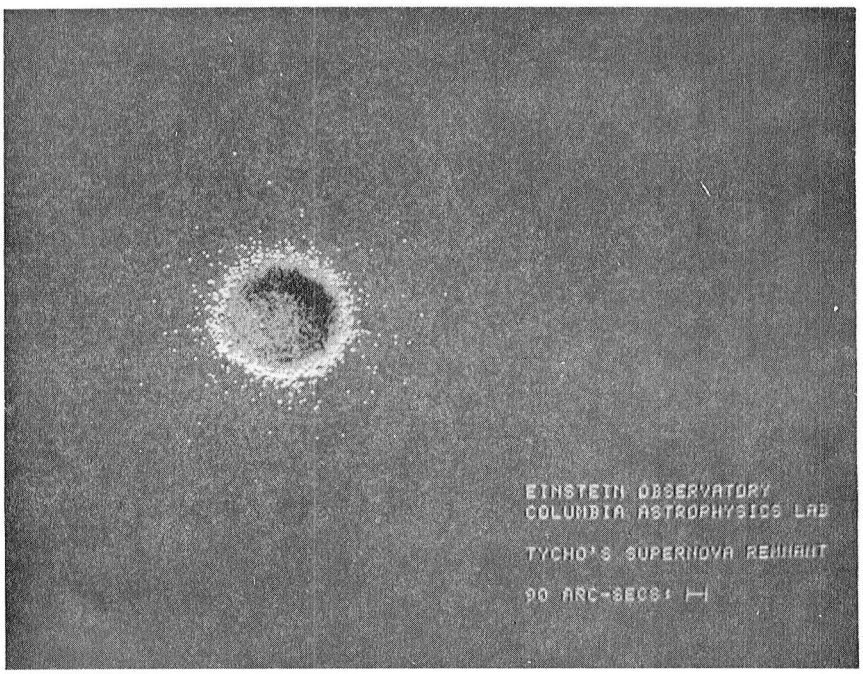

Figure 3. Tycho's supernova remnant.

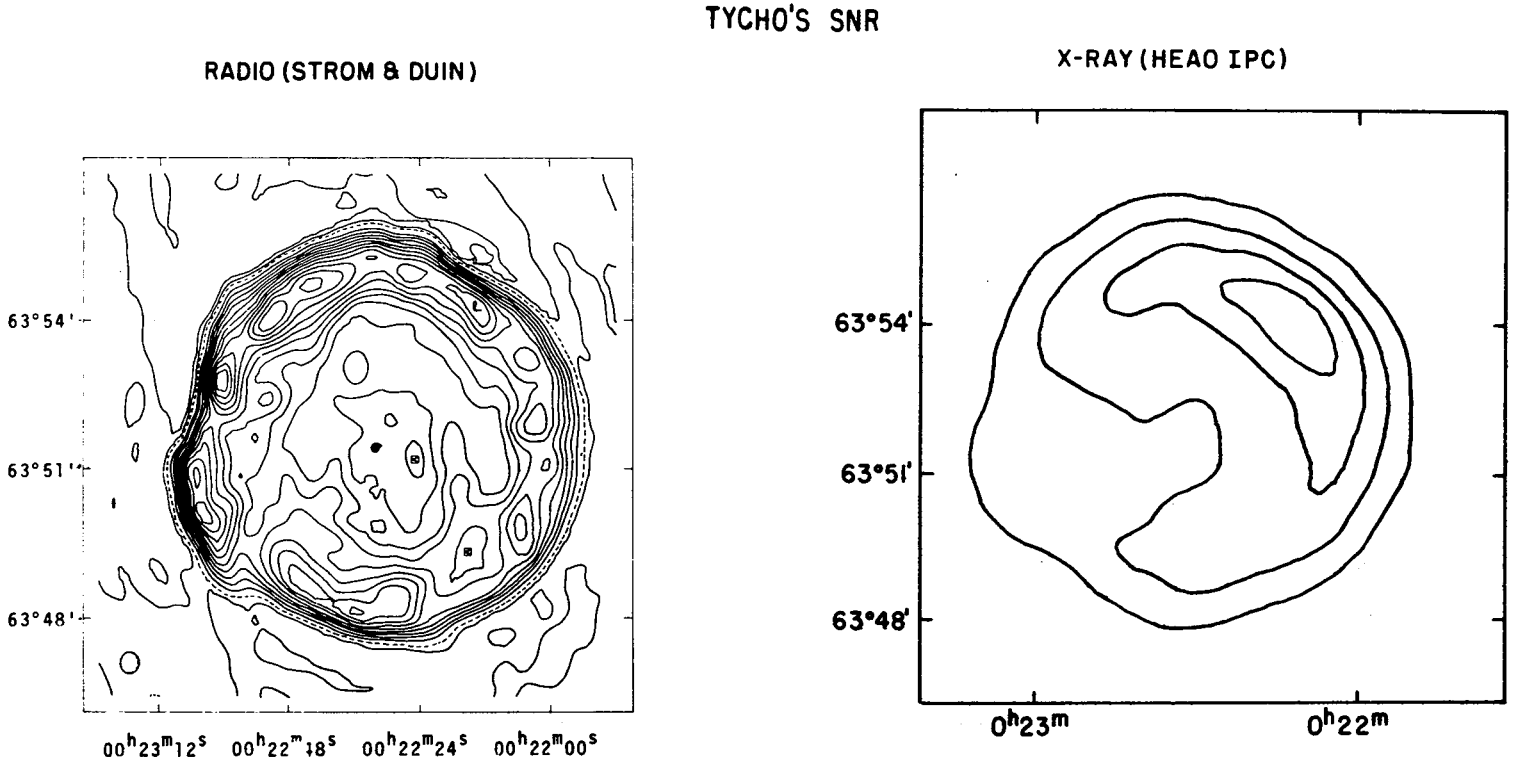

Figure 4. A comparison of radio and X-ray contours of Tycho's SNR. The radio map was taken from Strom and Duin (1973). The contour levels in the X-ray map correspond to approximately 1, 2, 3, and 4 counts $(1' \times 1')^{-1}$ s^{-1}.

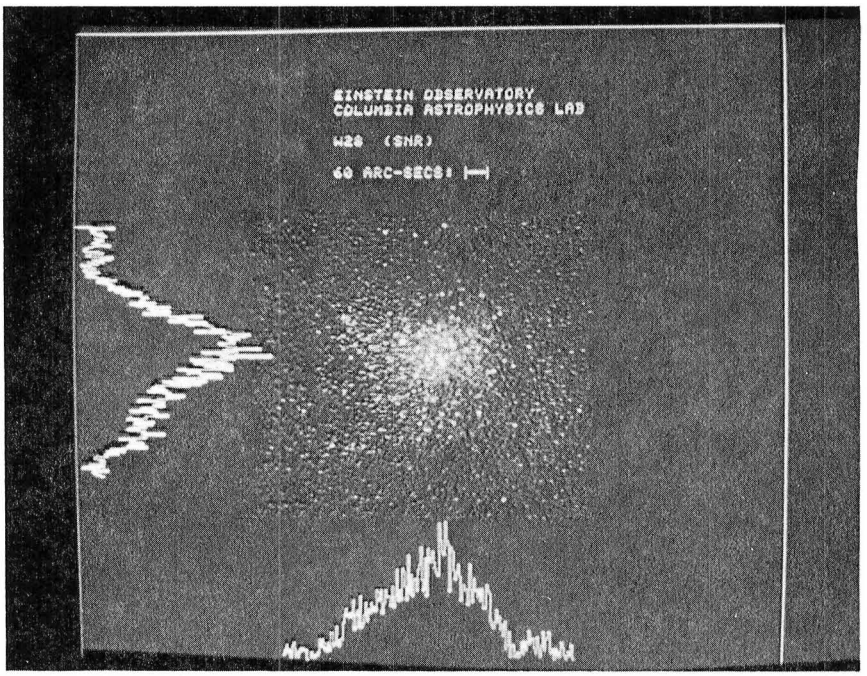

Figure 5. The supernova remnant W28.

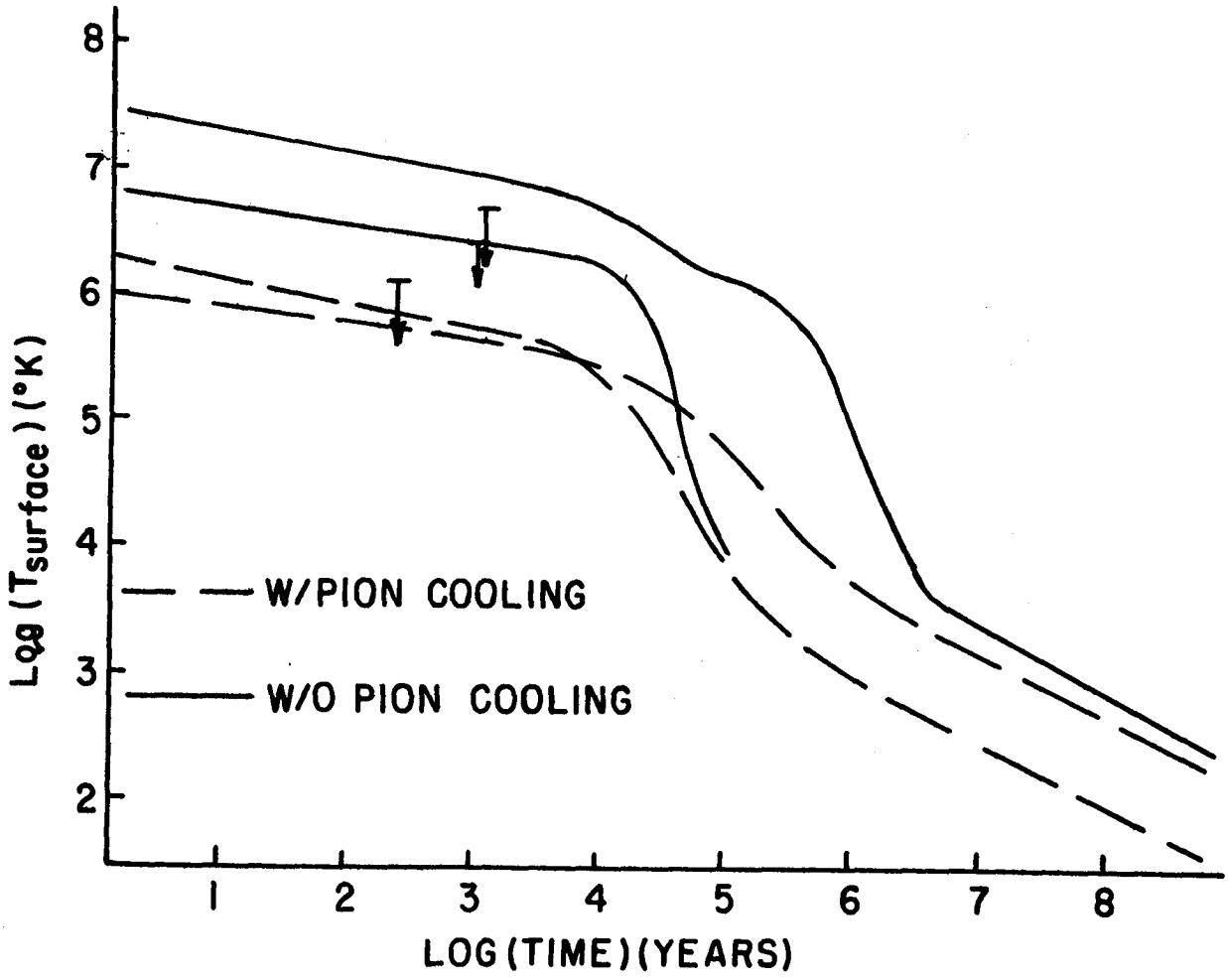

Figure 6. Cooling curves for neutron stars with limits derived from X-ray observations. The cooling curves shown represent the envelopes of various models for neutron star cooling without pion condensates (solid lines) and with pion condensates (dashed lines).

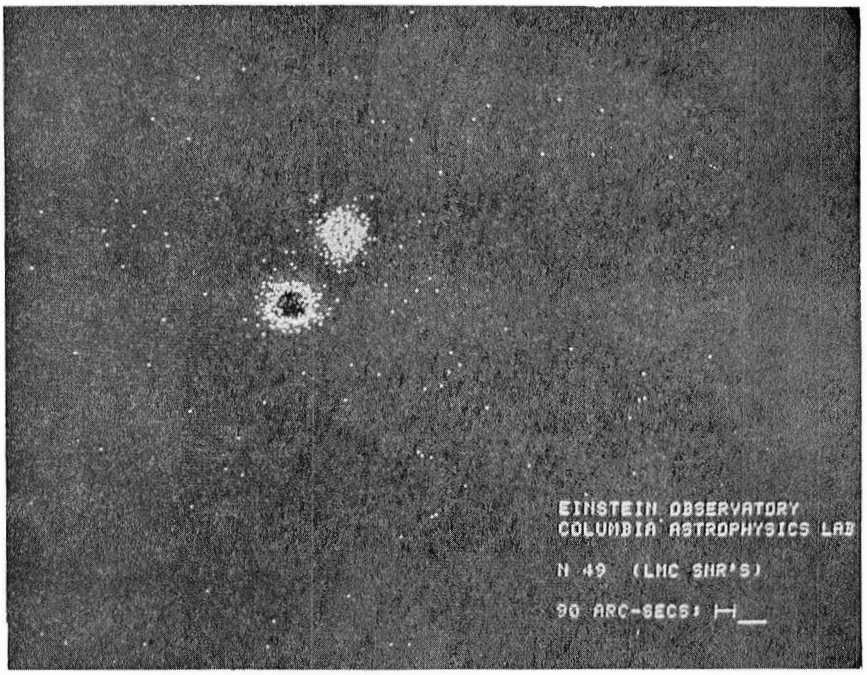

Figure 7. An IPC observation of two supernova remnants in the LMC. The remnant N49 in the southeast is approximately twice as bright as (N49) in the northeast.

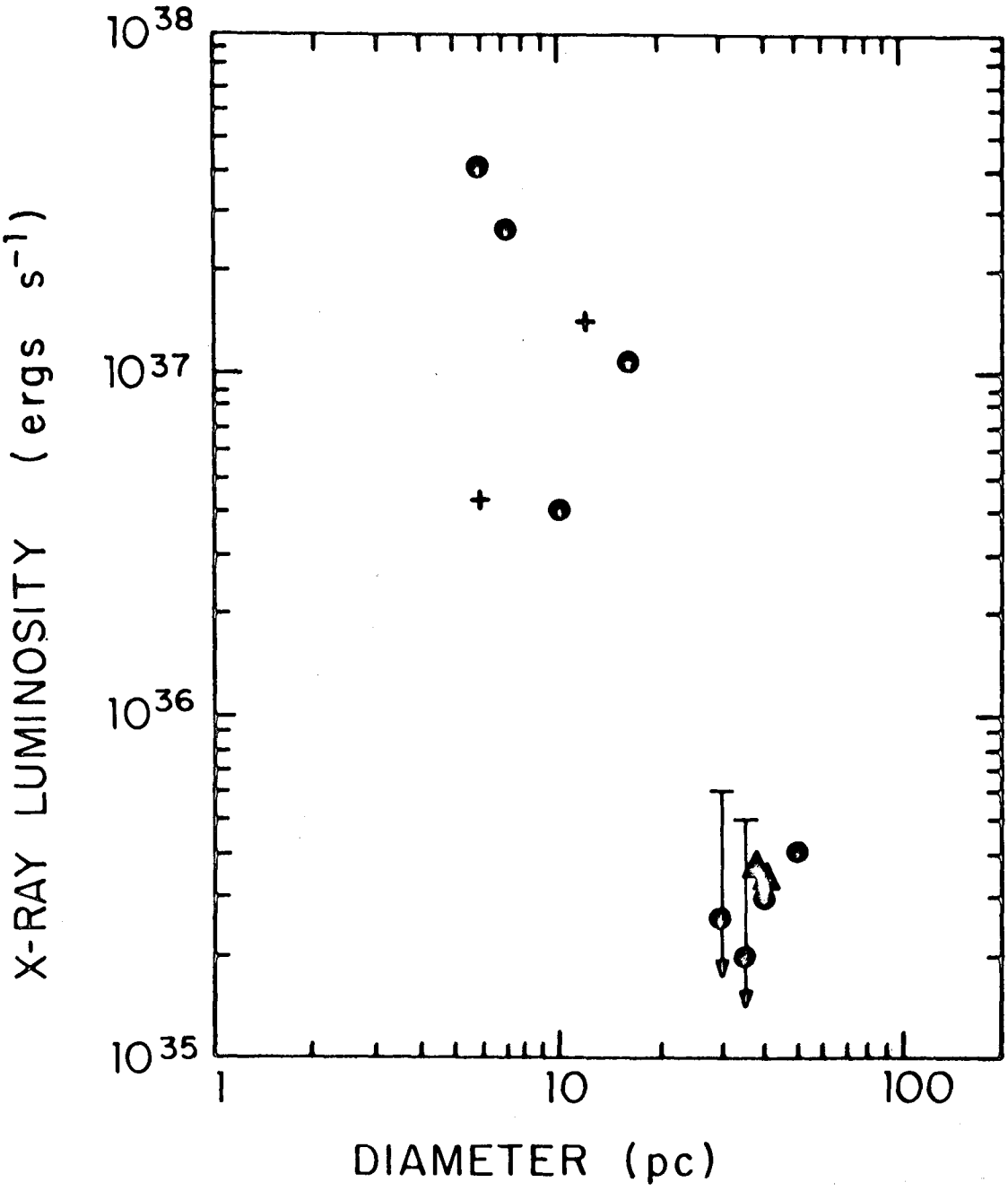

Figure 8. The X-ray luminosity of SNR in the LMC as a function of optical diameter. Diameters for N151B and N158A (+) were determined from a Σ - D relation by MC. The rest of the diameters were determined directly (MC = filled circles; DEM = filled triangles).

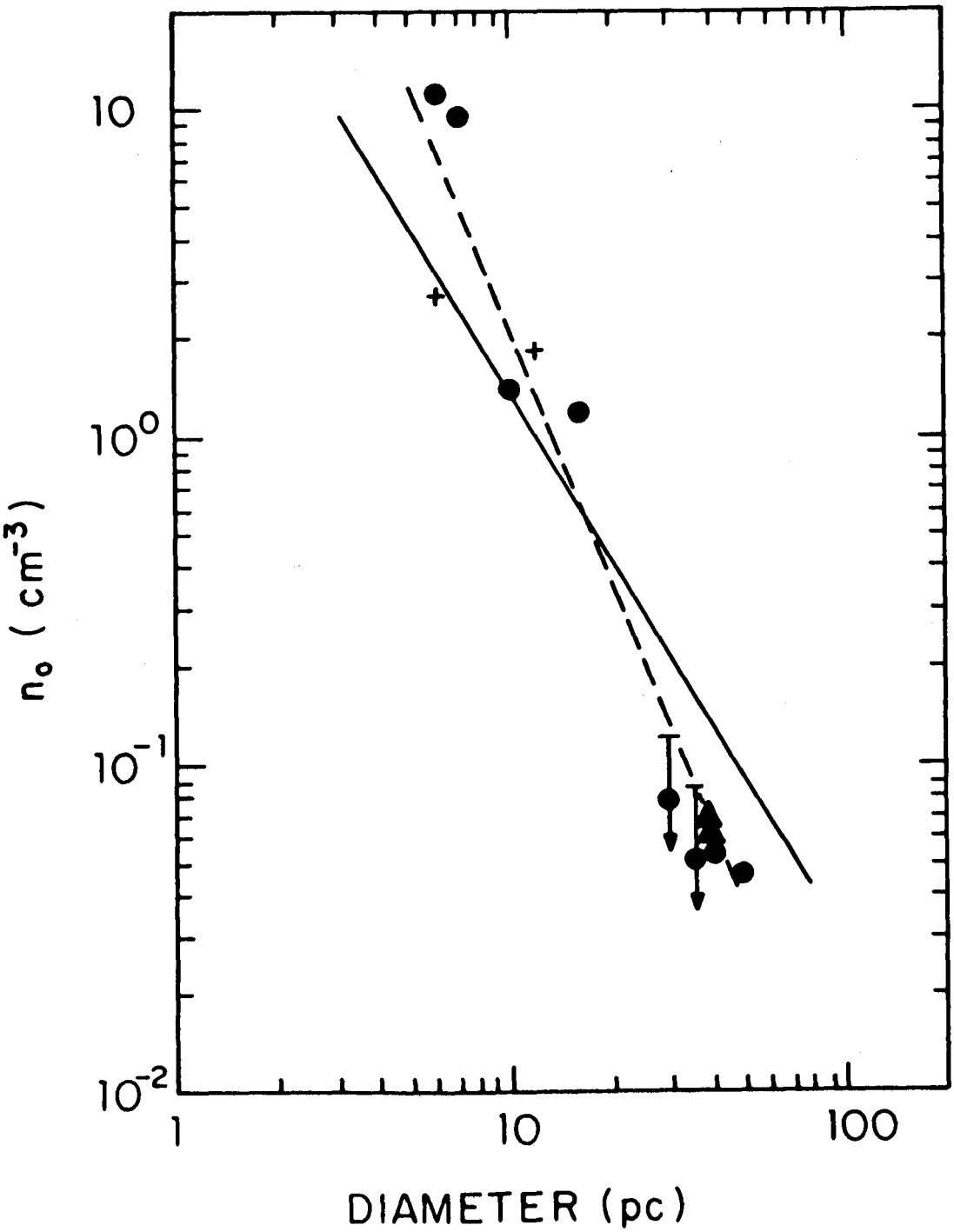

Figure 9. Derived values of n_o from the Sedov solutions for SNR in the LMC as a function of SNR diameter. The solid line indicates an approximate fit to a law, $n_o \propto D^{-5/3}$, as predicted by McKee and Ostriker (1977). The actual slope is better fit by a somewhat steeper law, $n_o \propto D^{-5/2}$ (dashed line). Symbols are as in Figure 8.

Figure 10. An IPC image of the 30 Doradus field. Sources are discussed in the text.